

# Ku-band/Ka-band Simulation & Testing of a 3D Printed Dielectric Lens Fabricated from Low-loss and Low-dk Resin

**CASE STUDY**

## INTRODUCTION

---

With a legacy of innovative antenna design, the Advanced Technology Group of Envistacom, LLC, recently spun off as the Apothym Technologies Group, LLC (or ATG), is always in search of new antenna technologies having the potential to advance the capabilities of warfighter, satellite, and terrestrial communications. This is why the engineers with ATG sought to evaluate Fortify's 3D printed low-loss and low-dielectric permittivity polymer resin for use in advanced antennas. With this technology Fortify engineers have been able to print extremely intricate and high resolution gradient index of refraction (GRIN) dielectric lenses that operate well at microwave/mm-wave frequencies. These lenses, impossible or extremely difficult to manufacture with traditional methods, can provide substantial antenna gain in a relatively compact shape and with minimal weight.

**This case study discusses the process from design, simulation, and testing of such a GRIN dielectric lens, and provides results that show the promise of this technology in cutting-edge communications systems.**

**“We have evaluated the Fortify lens technology and discovered that it is a very useful technique for realizing Luneburg lenses for various applications. ATG is excited about engaging with Fortify further and exploring the use of this technology in future solutions.”**

-Shawn Rogers, Ph.D., Sr. Phased Array Antenna Engineer, ATG.

## GRIN/LUNEBURG LENS DESIGN AND 3D PRINTING

The 3D printed GRIN dielectric lens discussed in this study is a Luneburg-style lens that uses graded dielectric layers to enhance the gain and directivity of an antenna feed placed at the center of the lens. Unlike other dielectric lenses, the high performance 3D printing process used to fabricate this lens is capable of using Rogers Radix™ material, which demonstrates low-loss ( $Df = 0.0043$ ) and low-dielectric constant ( $Dk = 2.8$ ), and can be printed as a single monolithic structure. Particular to this lens, the unit cells are structured as gyroids, and offer a balance between minimizing material, accurate recreation of the graded dielectric shells, and printability.

The spherical lens structure is divided into 6 shells, with varying dielectric constant and radius in order to optimally approximate the ideal Luneburg lens design which has a continuously graded dielectric constant profile. The goal of the lens is to enhance the antenna gain/directivity without significantly degrading the antenna efficiency when directly fed by a waveguide. The effect of the lens on the waveguide feed is to increase the effective antenna aperture size. In the transmit case, this is done by passing the electric and magnetic fields emitted from the antenna feed into the RF lens in such a way that the fields are properly phased as they exit the lens on the opposite side.

If the lens is appropriately designed and fabricated, the result is the output of a planewave outside of the lens on the side opposite the feed and an efficient use of the entire potential cross-sectional aperture of the lens. For performing system level design trade studies, engineers use the well-known area gain formula augmented by efficiency as presented in equation 1 where  $G$  is the antenna gain in dBi,  $\lambda$  is the free-space wavelength,  $A$  is the area of the circular cross section of the lens through its center, and  $\eta$  is the decimal form of the efficiency of the lens. The lens efficiency includes the effect

of dielectric losses and any deviations from uniformly illuminating the circular area cross section of the lens. As an example, if there are no dielectric losses and the aperture area is illuminated uniformly without any tapering then the lens would have an efficiency of 100%. While engineers always strive to design lenses with the best efficiency, practical values can be between 50% and 85% depending on a number of factors, including frequency of operation, lens size, and feed design.

Equation 1

$$G = 10 \log_{10} \left( \frac{4\pi A}{\lambda^2} \eta \right)$$

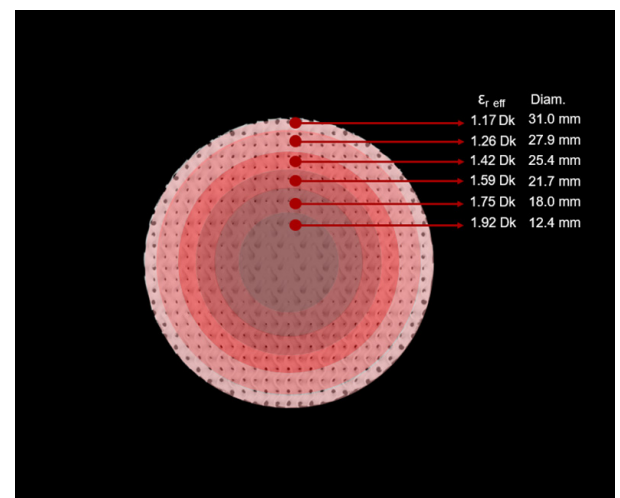


**Figure 1:** The six spherical shells of the Luneburg lens design with varying dielectric constant and diameter.

## EM SIMULATION OF LUNEBURG LENS WITH RECTANGULAR WAVEGUIDE FEED

In order to better understand and begin the process of developing models and methods for refining dielectric lens designs produced with this process, the current design is simulated in Ansys HFSS (High Frequency Structure Simulator) which is a finite element method for solving Maxwell's equations. For the purpose of modeling a real-world antenna feed system, the model includes a WR-28 waveguide feed with flange.

Given the structural complexity of the model and the high maximum frequency of the simulation (39 GHz), several model complexity reduction methods are used. One of these methods is the modeling and simulation of the lens as 6 solid homogeneous shells each having a unique dielectric constant as indicated in Figure 1 and with a dielectric loss tangent of 0.0043. Simulating just the shell approximation of the lens allows for a significant reduction in mesh complexity which enables the problem to be solved.

The ATG engineers attempted to simulate a quarter of the lens comprised of the actual gyroid unit cells. However, the HFSS software was unable to successfully generate a first mesh of the complex lens and crashed after five hours with a non-manifold edge geometry error. Another method for reducing simulation time and computer memory usage is to take advantage of the spherical lens' intrinsic symmetry and simulate only a quarter of the lens. Using quarter-model symmetry reduces the model volume by a factor of four which in turn reduces the number of unknown field quantities ( $N$ ) to be solved by a factor of four. Solving a system of linear equations has a time complexity of at most  $O(N^3)$  (on the order of  $N^3$  operations in the common big  $O$  notation for expressing time complexity). Since the finite element method matrix is sparse, it will have a time complexity less than this but the exact value is dependent on the equations and problem being solved.

From anecdotal experience with the finite element method for electromagnetics, this complexity is estimated to be  $O(N^2)$ . Therefore, in theory, reduction the problem volume by a factor of four reduces the solve time by a factor of 16. A simple comparison example was constructed from the described lens problem at one frequency (35 GHz) and for only one adaptive pass in HFSS Version 2021R2 and a run on a computer with two 8-core Intel(R) Xeon(R) Gold 6144 processors running at 3.50GHz. (Due to purchasing the basic multicore HFSS licensing option, only four cores are utilized during these simulation examples.) The quarter model resulted in 47,588 tetrahedra and solved within 131 seconds while the full model resulted in 181,817 tetrahedra and solved within 2143 seconds. Thus, the speed improvement for this example is a factor of 16.35. Note that these comparisons are for total run times, not only matrix-solve time.

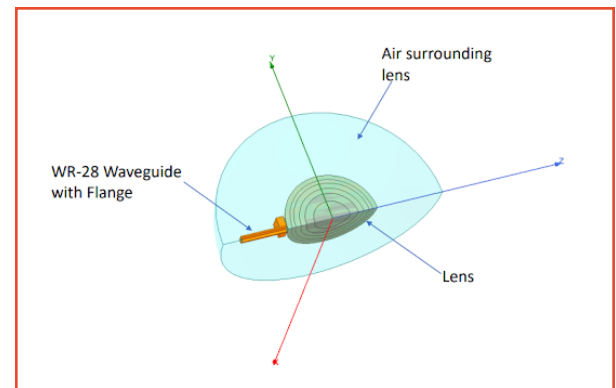


**Figure 2:** Quartered cross-section of the 6-shell approximated lens design with a WR-28 waveguide/ flange and surrounding air.

The WR-28 waveguide and flange are also simulated without the lens to confirm the model performance of the waveguide.



## ANTENNA TEST OF WR-28 WAVEGUIDE FEEDING FORTIFY LUNEBURG LENS

The practical testing of the 2.44" aperture GRIN lens requires RF absorbing materials, a measurement horn antenna (which is a standard-gain horn in this case), a separate standard-gain horn (not shown) for measurement calibration, and a fixture to hold the lens and WR-28 coaxial-to-waveguide adapter in precision alignment. A coaxial-to-waveguide adapter is used to feed the lens and is connected to the Rohde & Schwarz (Model #ZNB-40) vector-network analyzer (VNA) through common coaxial cable with 2.92mm connectors. Proper alignment can be obtained by making slight adjustments to the positioning of the waveguide relative to the lens until maximum gain is measured during the setup for broadside gain.

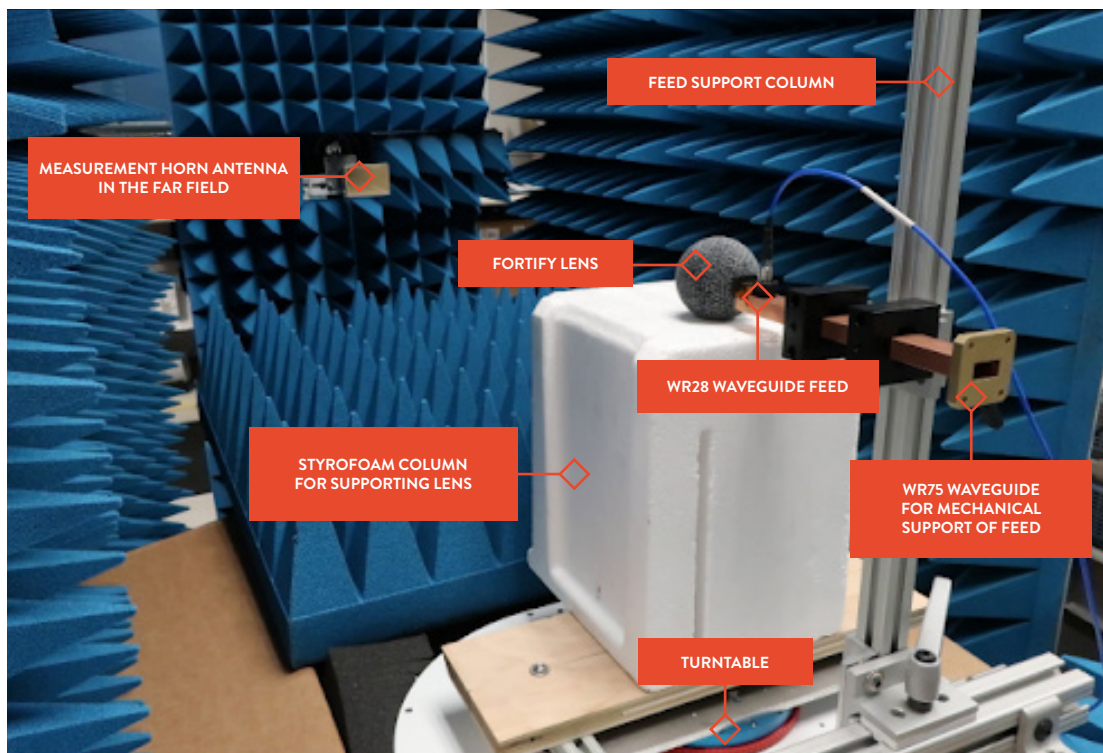


**Figure 3:** The practical test setup of the Fortify Luneburg Lens fed by a WR-28 coaxial to waveguide adapter during Ka-band measurements.

4.

A Styrofoam column with a dimple at the top is used to hold the lens in place above a turntable that enables the capture of pattern cuts. The Styrofoam supporting column eliminates the need for another dielectric or metal support structures near the lens which could change the antenna gain pattern of the lens and would deviate from the simulated model causing more questions to arise when measurements and simulations are compared. The lens is centered in-line with the rotational axis of the turntable. The waveguide and spherical antenna are placed along an axis of alignment with the measurement horn antenna, while RF absorbing materials are placed on all sides around the test area. In this case, the top was not covered with RF absorbing materials and there are some gaps in the coverage of the absorbing materials, so the chamber isn't completely anechoic. The reflections observed in the data may be a result of this.

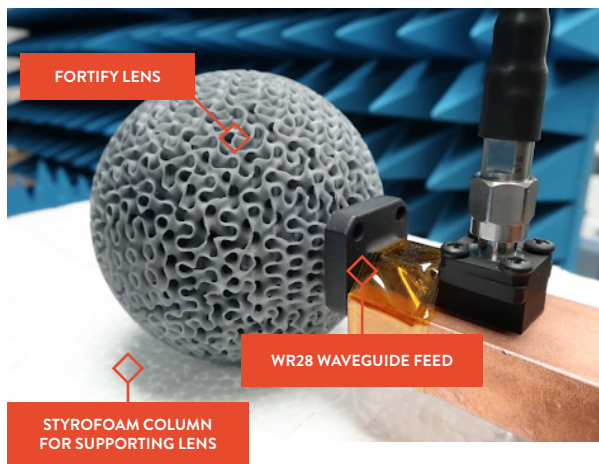


**Figure 4:** Close-up photograph of the WR-28 coaxial-to-waveguide adapter used in Ka-band measurements for feeding the Fortify 2.44" Luneburg lens, which is fabricated using a high resolution gyroid structure.

Measurements of the open-ended coaxial-to-waveguide adapter are also taken to provide a comparison of the performance of the coaxial-to-waveguide adapter as a feed for the luneburg lens. In a similar way, the lens is also measured in the Ku-band with a WR-75 coaxial-to-waveguide adapter as a feed.

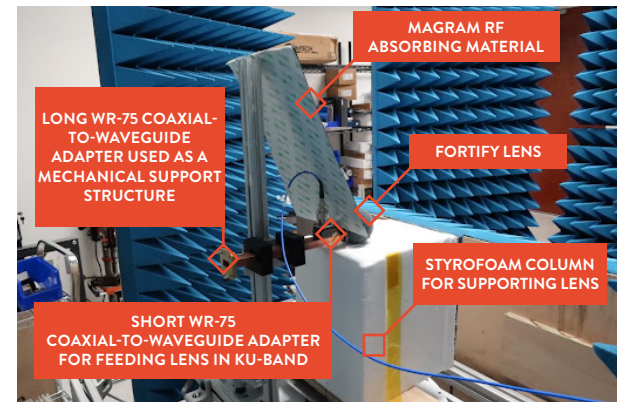


**Figure 5:** A picture of the test setup for the Ku-band measurements.

## RESULTS & DISCUSSION

The following sections are devoted to presenting and discussing the results of the Ka-band and Ku-band testing of the 2.44" Luneburg lens provided by Fortify and how these measurements compare to the simulation of a simplified model of the lens.

### KA-BAND SIMULATION VS. MEASUREMENTS

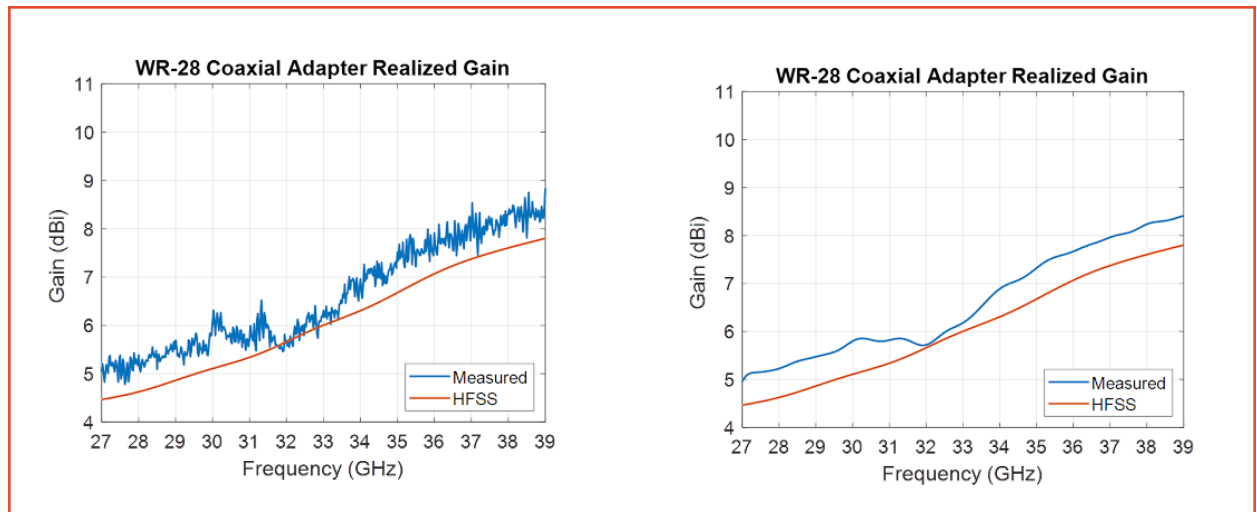


**Figure 6:**

- (a) the realized gain of the WR-28 coaxial-to-waveguide adapter
- (b) with time-gating to reduce the impact of the reflections in the test room.

Initially, the WR-28 coaxial-to-waveguide adapter is measured without the lens. The resulting realized gain plot (Figure 6a) includes a significant amount of reflections, likely from any gaps in the RF absorbing material chamber, including the uncovered top of the improvised chamber. A time-gating method using a Hamming window is implemented in MATLAB is used to mitigate the reflection response in the measurements (Figure 6b). It can be observed that the WR-28 coaxial-to-waveguide adapter exhibits realized gain within a 0.5 dB of the HFSS simulation.

Though this measurement does provide confidence in the simulation approach, further development of the simulation or optimization of the test chamber could improve this matching of simulation and measured gain response.

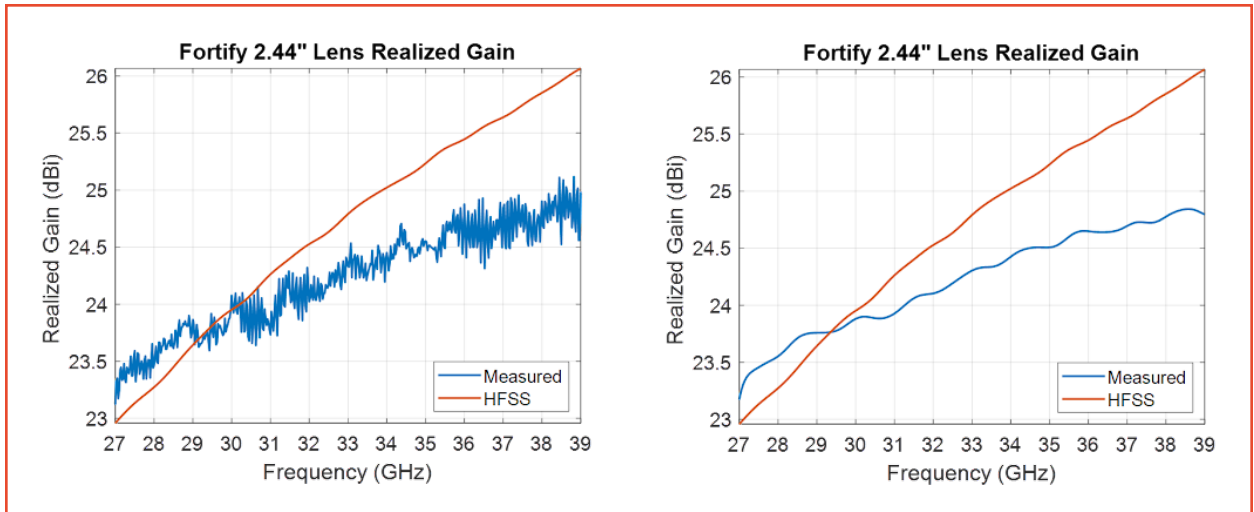


**Figure 7:**

(a) the realized gain plot of the Fortify 2.44" GRIN Lens.

(b) with time-gating to reduce the impact of reflections in the test room.

It can be observed by the realized gain plots in Figure 7 that the gain of the actual 2.44" lens is greater than the HFSS simulation until ~29.5 GHz, where it appears to decay faster than that predicted by the HFSS model. Given the model simplification methods used in the simulation, it is possible that simulation of the actual gyroid GRIN lens structure provided would yield a simulation that more accurately matches the results.

The aperture efficiency of the spherical antenna - this time calculated as a percentage instead of in decimal form - is calculated by comparing the realized gain to the aperture can provide equation 2.

**Equation 2:** Where A is the area of a circular cross section of the sphere through its center,  $\lambda$  is the wavelength, and  $G_m$  is the measured antenna gain on a linear scale (not in dBi).

$$\eta \text{ (in \%)} = G_m \frac{\lambda^2}{4\pi A} \cdot 100$$



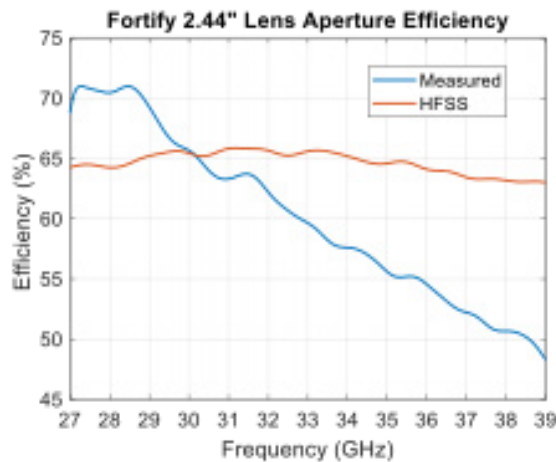


**Figure 8:** Measured versus simulated aperture efficiency of the 2.44” 3D printed lens with WR-28 coaxial-to-waveguide adapter.

The plot in Figure 8 shows that the 2.44” dielectric lens prototype is over 65% efficient to ~30 GHz, where the efficiency begins to decay much faster than the HFSS simulation. This follows the results observed with the realized gain data.

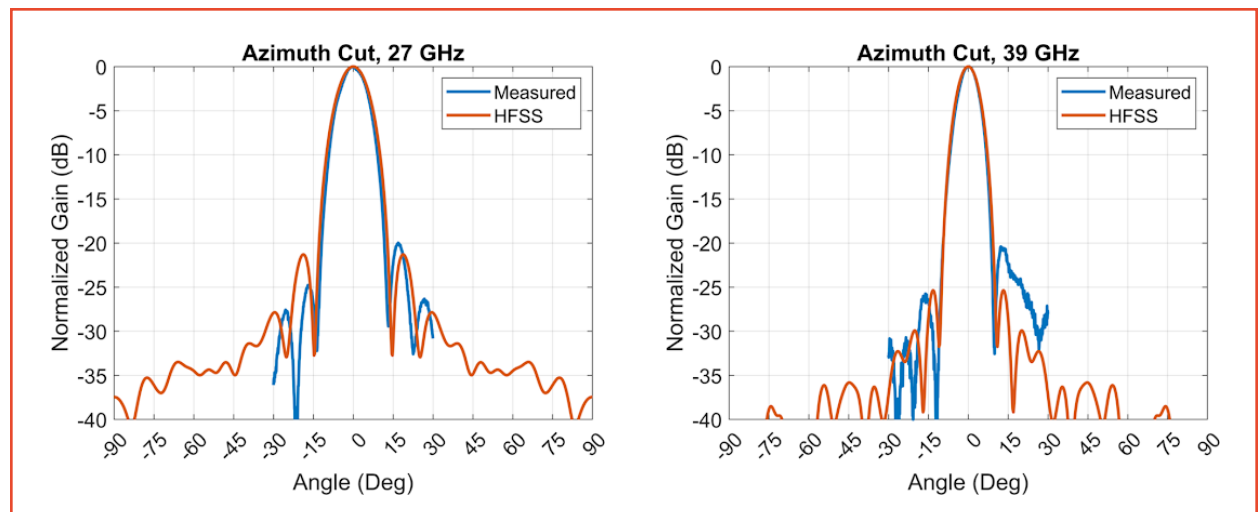


**Figure 9:** 2.44” dielectric lens pattern cuts normalized to peak gain at (a) 27 GHz and (b) 39 GHz.

In the normalized pattern cuts in Figure 9, it can be observed that there is very good agreement between the HFSS simulation and the measured lens results. However, there is a slight asymmetry in the sidelobes of the measured pattern cuts which could be attributed to the feed behind slightly misaligned from the exact center center of the lens. Nevertheless, the agreement of the measured and calculated patterns in the main beam is excellent.

## KU-BAND SIMULATION VS. MEASUREMENTS

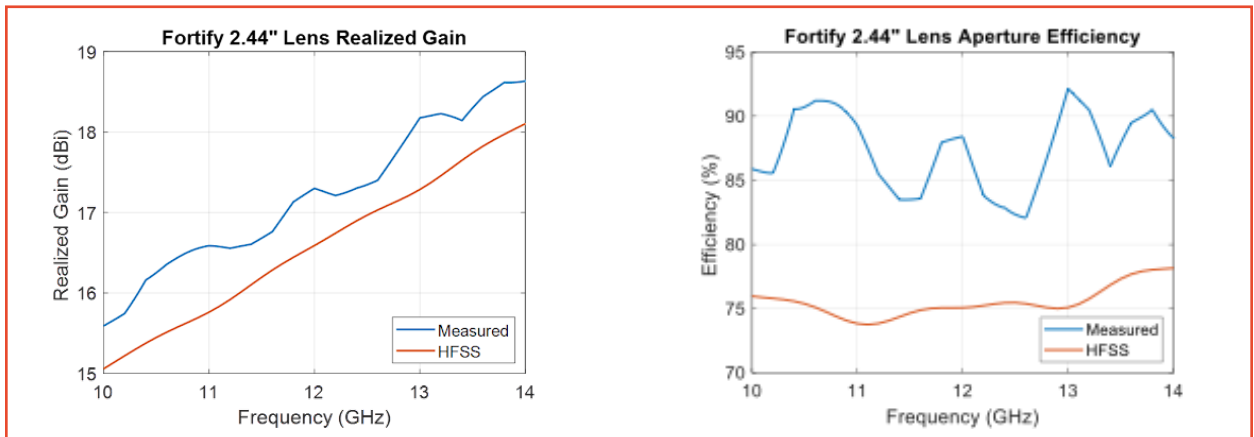


**Figure 10:**

(a) realized gain of the Fortify 2.44" dielectric lens both simulated and measured.  
 (b) lens aperture efficiency of the 2.44" lens both simulated and measured.

The results (Figure 10a) of the Ku-band simulated and measured realized gain demonstrate a close match between the simulation and measured data, with the exception of a slight positive offset of the measured waveguide fed lens gain. This positive offset is also observed in the lens aperture efficiency results in Figure 10b.

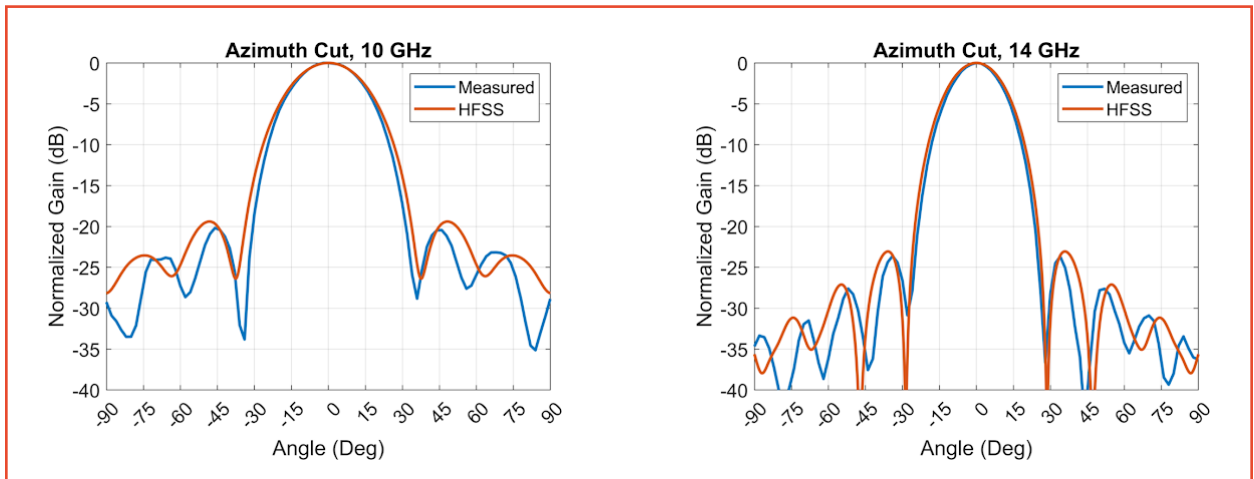


**Figure 11:** 2.44" dielectric lens pattern cuts normalized to peak gain at (a) 10 GHz and (b) 14 GHz.

Similar to the Ka-band data, the pattern cuts normalized to peak gain match well between the simulated and measured results. Unlike the Ka-band measured results, the 10 GHz and 14 GHz pattern cuts in Figure 11 exhibit very little asymmetry. This underscores an observation that measurement challenges increase with increasing frequency.

## CONCLUSION

Even with the coarse approximation made for the lens simulation model, the agreement between the HFSS simulations and measurements is reasonable and validates the overall approach of the lens design and fabrication method. The initial positive evaluation of the Fortify lens technology indicates that it will find many applications in various antenna products. With further optimization of the lens design and simulation strategy, it is likely that the lens performance can be further enhanced and the simulation model could be made to better match real-world outcomes. For some applications, the Ku-band certainly, and possibly the Ka-band performance to 38 GHz with efficiency above 50% is already adequate and the compact size and low weight of the GRIN lens is advantageous.

### ABOUT APOTHYM TECHNOLOGIES GROUP, LLC

Founded in 2022, Apothym Technologies Group (ATG) delivers products and capabilities that enable ubiquitous and secure wireless connectivity. Those solutions are derived from the company's focus on developing a transport virtualization platform and advanced multi-beam, multi-frequency antenna technologies. ATG is headquartered in Peachtree Corners, GA, with an additional research and development center in Frederick, MD.



### ABOUT FORTIFY

Fortify is transforming the 3D printing industry with its patented DCM (Digital Composite Manufacturing) platform. DCM delivers new levels of additively manufactured part performance by introducing functional additives to photopolymers. By combining a deep understanding of material science with high performance mixing, magnetics, and polymer physics, Fortify is able to produce custom microstructures in high-resolution 3D printed parts. The company is currently focused on applications ranging from injection mold tooling to high performance end-use parts with unique mechanical and electromagnetic properties. Founded in 2016 and based in Boston, Fortify technology enables material properties and components unattainable using other additive or traditional manufacturing processes. For more information, visit [www.3dfortify.com](http://www.3dfortify.com).



7.

---

## RESOURCES

---

[1] [“https://rogerscorp.com/advanced-electronics-solutions/radix-printable-dielectric](https://rogerscorp.com/advanced-electronics-solutions/radix-printable-dielectric)



WWW.3DFORTIFY.COM  
SALES@3DFORTIFY.COM  
75 HOOD PARK DRIVE, BLDG 510, BOSTON, MA 02129